Nascent Rotational Distributions of MgH in Reaction of $Mg(4s^1S_0)$ with H_2 and HD

Dean-Kuo Liu*[a] (劉定國) and King-Chuen Lin[b] (林金全)
[a]*Institute of Atomic and Molecular Sciences, Academia Sinica, P.O. Box 23-166, Taipei, Taiwan 106, R.O.C.*
[b]*Department of Chemistry, National Taiwan University, Taipei, and Institute of Atomic and Molecular Sciences, Academia Sinica, P.O. Box 23-166, Taipei, Taiwan 106, R.O.C.*

The nascent rotational distributions of $MgH(X^2\Sigma^+, v'' = 0,1)$ resulting from the reaction of $Mg(4s^1S_0)$ with H_2 and HD have been determined by using the laser pump-probe technique. Like the case of $Mg(^1P_1)$, the distributions appear to be bimodal which peak mainly at high N(26) with minor peaks at low N(6). There are no apparent differences when the escaping mass is doubled. The similarity between product rotational distributions from the 4S state and those from the 3P state, and no evidence of a kinematic isotope effect, reveal that a harpoon-type mechanism may be operative. Our ab initio calculations reveal that in the entrance channel on the 3^1A_1 surface in C_{2v} symmetry or $^1\Sigma^+$ surface in $C_{\infty v}$ symmetry for 4S state, the reaction may take place via a series of non-adiabatic curve crossings with the ionic $Mg^+H_2^-$ potential surface.

INTRODUCTION

In the field of chemical reaction dynamics, if fewer particles are involved in the reaction, it becomes easy to control the experimental conditions and to consider only a few dynamical parameters used in the surface calculation. By combining the calculated and experimental results, the detailed behaviors of reaction dynamics can be understood.

The simplest three-atom reaction is $H + H_2$ and its isotopic variants. Next in order of complexity are the set of reactions involving two hydrogen atoms. For the reaction $Mg(3p^1P_1) + H_2$, Breckenridge and Umemoto[1] found that the nascent rotational distributions of product $MgH(X^2\Sigma^+, v'' = 0,1)$ were bimodal. They proposed two parallel competing mechanisms, Mg-insertion and H-abstraction, which were responsible for high-N and low-N distributions, respectively. In the next year, McCaffery *et al.*[2] probed the intermediate complex MgH_2 using matrix isolation at 12 K and identified it to be a linear structure H-Mg-H. On the other hand, Chaquin *et al.*[3] have conducted the potential energy surface calculations for the $Mg(3p^1P_1) + H_2$ system. Their calculated results showed that in the C_{2v} collision geometry, the reaction could happen along the attractive surface 1^1B_2, and that in the $C_{\infty v}$ collision geometry, there would be an 1.8 eV energy barrier in the entrance channel for the $^1\Sigma^+$ surface and an 1.7 eV for the $^1\Pi$ surface. In 1987, Breckenridge and Wang[4] found that the distributions of product $MgH(v'' = 0)$ in the reaction of $Mg(3p^1P_1)$ with H_2 and HD are similar and that both display bimodal behavior. They considered that both the predominant "high-N" and the minor "low-N" components of the distributions resulted from insertion of $Mg(3p^1P_1)$ into the H-H bond. Later, Lin and Huang[5] found that the $MgH(v'' = 0)$ product rotational distributions were temperature invariant, which further supported the insertion mechanism for the bimodal distributions.

Recently, we presented more detailed information on the vibrational population distributions of MgH and conducted a two-dimentional potential energy surface (PES) calculation for the reaction $Mg(3p^1P_1) + H_2$.[6,7] The resulting PES's information revealed the possibility of a nonadiabatic crossing between the excited 1^1B_2 PES and the ground 1^1A_1 PES. The intermediate near the surface crossing, which follows directly the dissociation coordinate of the Mg-H distance, may have MgH produced in low rotational states and preferentially in the vibrational ground state $v'' = 0$. In contrast, the intermediate which is attracted to pass through a linear geometry may lead to both rotational and vibrationally excited MgH.

In the present work, we employ the pump-and-probe technique to determine the nascent rotational distributions of MgH produced in the reaction of Mg(4S) with H_2 and HD. Furthermore, it is interesting to see whether the rotational distributions for the current system are different from those for the $Mg(3P) + H_2$ case.

EXPERIMENTAL

The pump-and-probe technique used in this work has been illustrated previously.[6-8] Briefly, the pump-and-probe technique employed two dye lasers with a pulse width of 8 ns and a spectral resolution of ≤ 1 cm^{-1}. The first dye laser,

pumped by an Nd:YAG (GCR3, Spectra-Physics) laser, was operated at 459.7 nm and used as a PUMP beam to bring the Mg atom to its electronic excited 4S state via a two-photon absorption. A methanol solution of Coumarin 460 was used. The PUMP laser energy was controlled within 1-3 mJ/pulse in order to avoid a further multiphoton absorption. The second dye laser, pumped by another Nd:YAG (DCR-2A, Quanta-Ray) laser, was used as a PROBE beam for probing the internal energy distributions of the MgH product via its $A^2\Pi$-$X^2\Sigma^+$ electronic transition. The nascent rotational state distributions can be obtained by carefully controlling the pulse delay time between the two involved laser beams and also the H_2 or HD pressure in the bulk. The PROBE laser energy was attenuated to be less than 100 μJ/pulse to avoid optical saturation. Coumarin 500 and Coumarin 540A were used for probing the MgH(0,0) [(v′,v″) notation is used] and MgH(0,1) bands, respectively. Magnesium metal (99.9% purity, Merck) was deposited in a crossed heat-pipe oven operated at 720 K, corresponding to a Mg vapor pressure of 10^{-2} torr. The colliding partner H_2 or HD was regulated at a typical pressure of 4 torr. The laser induced fluorescence (LIF) was observed in the direction perpendicular to the laser beam axis and collected by means of two lenses onto a monochromator (SPEX1680), which was set to have a bandpass of 14.4 nm and was used as an interference filter. The center wavelength of the grating was set at 560 nm and 517 nm for the $v' = 0 \rightarrow v'' = 1$ and $v' = 0 \rightarrow v'' = 0$ transitions, respectively. The transmitted LIF signal was collected by an attached photomultiplier tube (EMI9658). The electric signal was processed by a boxcar integrator (EG&G 4420) and the averaged results were stored by a microcomputer for further data treatment.

Since the rotational spectra of the MgH(0,0) and MgH(0,1) bands overlap severely in the bandhead region for N = 11-20 and N = 8-14,[9-12] respectively, we had to determine the nascent rotational distributions by spectral simulation. For the MgH(0,0) band, the P branch was well resolved up to N = 30, but for the MgH(0,1) band, both the Q and R branches overlapped with the P branch nearby $N \leq 20$ and making the spectral assignment troublesome. For clarity, we chose the P branch to determine the rotational distributions.

The rotational distributions of the $v'' = 0$ state were determined by measuring the excitation spectrum of the (0,0) band via the fluorescence detection of the (0,1) band. In contrast, for detecting the population in the $v'' = 1$ state, the (0,1) band is excited and then the (0,0) band is monitored. Although the Franck-Condon factor for $v'' = 1 \rightarrow v' = 0$ is 10 times smaller than $v'' = 0 \rightarrow v' = 0$,[13] the total transition probabilities for $v'' = 0$ and $v'' = 1$ are the same. Therefore, it is not necessary to take into account the Franck-Condon factor for correction.

The radiative relaxation for the 4S → 3P transition of Mg atom gives rise to a spontaneous emission coefficient of 2.6×10^7 s^{-1}, corresponding to a lifetime of 39 ns. During the present adopted delay time of 10 ns adopted, a < 25% population contribution of MgH may result from the relaxed 3P state. In order to assure that the measured MgH distributions are nascent and that the product contribution associated with the process of collisional relaxation is negligible under our experimental conditions, we shortened the delay time and found that the bimodal feature of the MgH distribution persisted without any significant change.

RESULTS

Rotational and vibrational spectrum

Fig. 1 and Fig. 2 present portions of the nascent rotational spectra of the $MgH(X^2\Sigma^+)$ $v'' = 0$ and $v'' = 1$, respectively, which were produced from the reaction of $Mg(4s^1S_0)$ with H_2. Fig. 3 and Fig. 4 portray their rotational populations derived from the P_1 branch. By comparing these rotational distributions with those obtained for the $Mg(3p^1P_1)$ + H_2 case,[5-7] which are also shown in the same figure, we found surprisingly that these distributions coincide with each other despite the different exothermic energy and atomic orbital symmetry involved. This similarity can be explained appropriately if the harpoon-type mechanism is operative. Fig. 5 presents nascent rotational distributions of $MgH(X^2\Sigma^+)$ $v'' = 0$ from the reaction of $Mg(4s^1S_0)$ with H_2 and those with HD. It can be seen that the MgH rotational distributions are essentially the same for the two cases. This isotopic invariance indicates that the bimodal distributions are due to the same reaction mechanism, an exit channel control reaction as that which occurs in the case of $Mg(3p^1P_1) + H_2$ reaction.[4]

ab initio PES calculation

To provide insight into the reaction pathway associated with the Mg(4s) state, we adopted the CIS (Single Excitation Configuration Interaction) scheme in the GAUSSIAN 92 package[14] to compute the potential energies of the excited states of $Mg(4s^1S_0$ and $3p^1P_1) + H_2$ as a function of the internuclear distance in a C_{2v} and $C_{\infty v}$ symmetry.[7,27] These calculations were done with basis sets at the 6-31G* level for the Mg and H atom. The computational results on both $MgH(^2\Pi$ and $^2\Sigma)$ and linear $HMgH(^1\Pi_g$ and $^1\Sigma_g)$ reveal

that their optimized bond lengths and total absolute potential energies were in agreement with those reported previously,[3] and in turn indicate that our methods are reliable. The H_2 bond was fixed at equilibrium distance 0.74 Å, while the internuclear distance between the Mg* and the center mass of H_2 was varied either in C_{2v} or in $C_{\infty v}$ symmetry. Each one dimensional potential energy surface (PES) was composed of twenty five points. Fig. 6 shows a part of the calculated results. For the 4S state, the $3^1A_1(C_{2v})$ and $3^1\Sigma^+(C_{\infty v})$ surfaces are attractive, but the $3^1A_1(C_{2v})$ surface has a slightly deeper potential well of 0.2 eV compared to 0.1 eV for the $3^1\Sigma^+$ surface. The PES's for the 3P state are similar to those of Chaquin *et al.*[3]

DISCUSSION

There is an tentative explanation for the subject reaction mechanism. Sevin and Chaquin[15] have conducted the ab initio calculation and suggested that the Na(4P) + H_2 reaction may proceed via a series of avoided and allowed surface crossings in C_{2v} geometry, coupling the excited 3^2B_2 with the 1^2B_2 surface by which the reaction may occur. The reaction is presumed to involve a rearrangement from triangular C_{2v} geometry to a linear H-Na-H intermediate which fragments to a product with excess rotational energy. Kleiber *et al*[16,17] have adopted this idea to the Na + H_2 full-collision case[16] and the half-collision case.[17] In Fig. 6 we can see that at the non-crossing point P, there exists a prob-

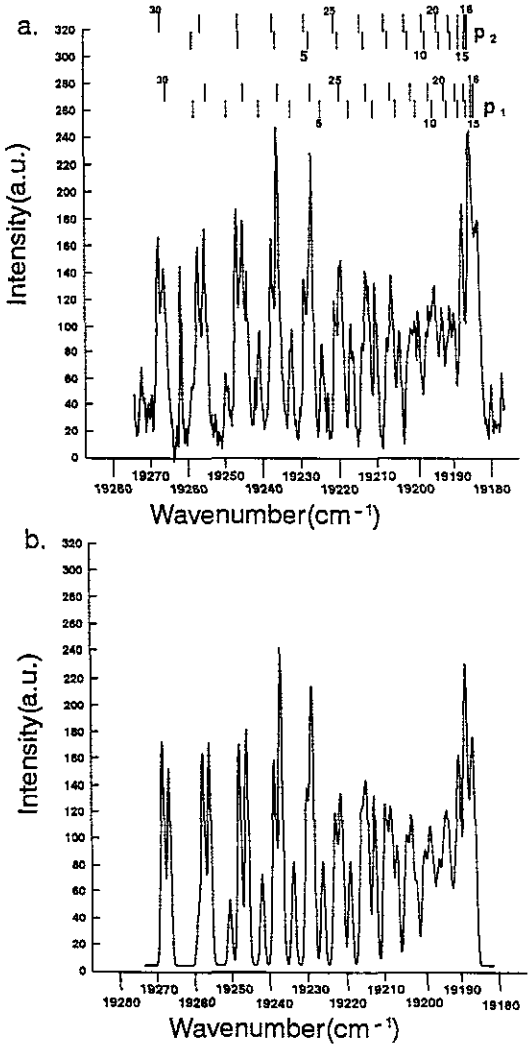

Fig. 1. (a) Portion of LIF spectra for the P_1 and P_2 branches in the (0,0) band of the MgH($A^2\Pi$-$X^2\Sigma^+$) transition. (b) Spectra by computer simulation of the same region. MgH($v'' = 0$) is a nascent product in the reaction of Mg(4^1S_0) with H_2.

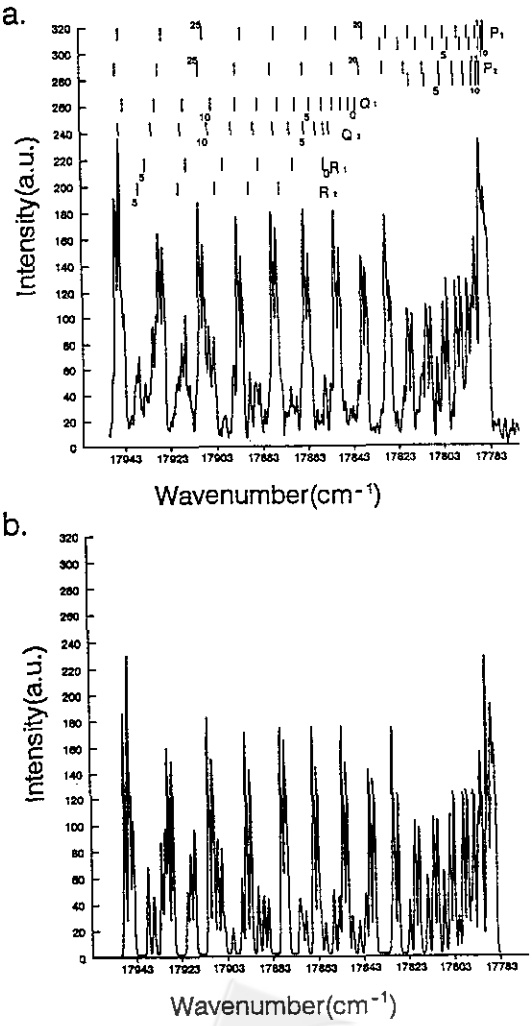

Fig. 2. (a) Portion of LIF spectra for the P, Q and R branches in the (0,1) band of the MgH($A^2\Pi$-$X^2\Sigma^+$) transition. (b) Spectra by computer simulation of the same region. MgH($v'' = 1$) is a nascent product in the reaction of Mg(4^1S_0) with H_2.

ability for valence electron jumping from the ionic Rydberg state 3^1A_1 to the valence state 2^1A_1. The 2^1A_1 state then couples with the 1^1B_2 state and a reaction may subsequently take place along this surface via non-adiabatic transition to produce the *MgH + H* product. However, the coupling strength between the quite repulsive 2^1A_1 surface and the attractive 1^1B_2 surface is expected to be weak, since on the 2^1A_1 surface there is a large repulsive force exerted on the Mg-H_2 intermediate and the moiety should break apart rapidly. A secondary collision seems to be required to produce MgH. Thus, this mechanism is not suitable for explaining the current system.

The rotational distributions are substantially consistent with those obtained in analogous studies of the $Mg(3p^1P_1) + H_2$ reaction. We propose the harpoon mechanism[18-20] to explain the similarity. This mechanism has been successfully applied to interpret the quenching rates of excited K atom by H_2 molecule,[21,22] in which the total quench-

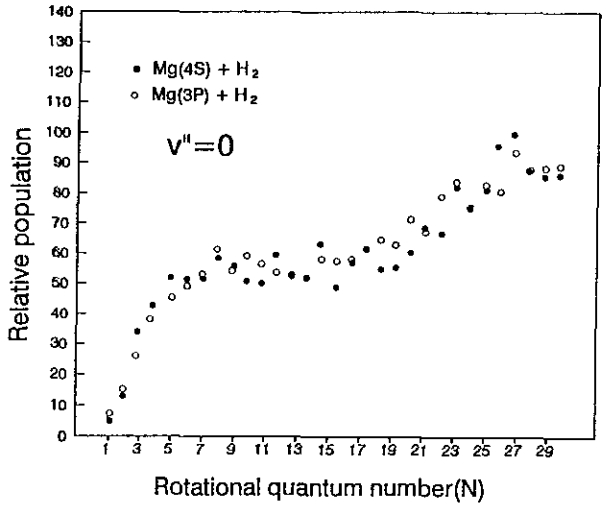

Fig. 3. Rotational population distributions of MgH(v″ = 0) from different atomic states of Mg. Solid circles and open circles denote the experimental results from the Mg(4S) and Mg(3P) states, respectively. All distributions have been normalized to the same scale.

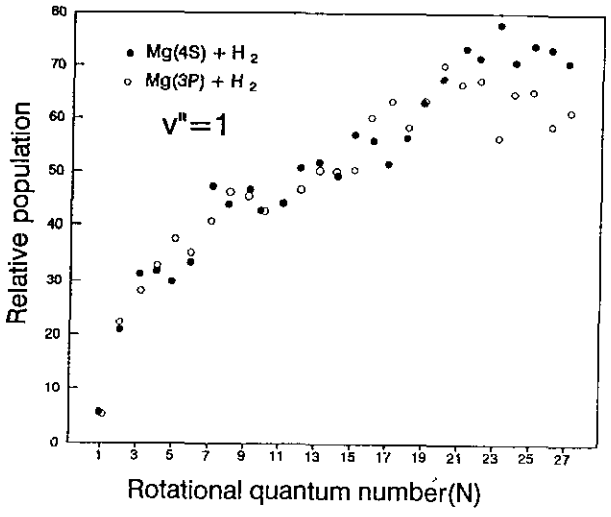

Fig. 4. Rotational population distributions of MgH(v″ = 1) from different atomic states of Mg. Solid circles and open circles denote the experimental results from 4S and 3P states, respectively. All distributions have been normalized to the same scale.

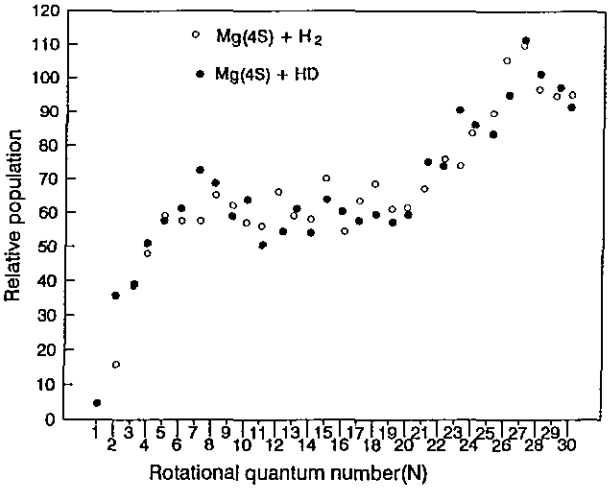

Fig. 5. Rotational population distributions of MgH(v″ = 0) from reaction of $Mg(4^1S_0)$ with H_2 and HD. Open circles and solid circles denote the experimental results for H_2 and HD, respectively. All distributions have been normalized to the same scale.

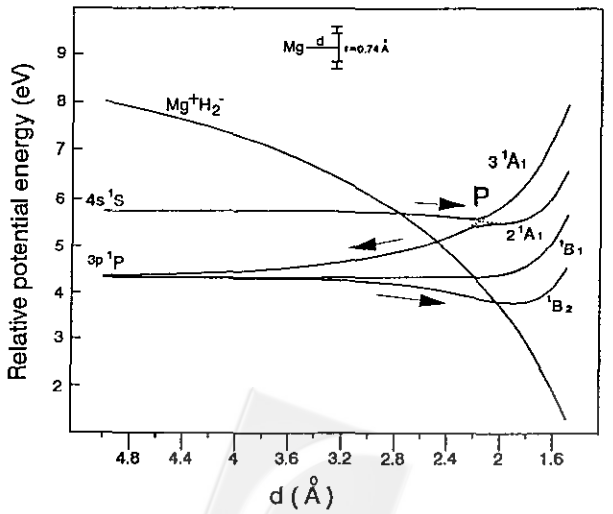

Fig. 6. Schematic drawing of intersecting potential curves to display the electron transfer reaction of $Mg(4s^1S_0) + H_2$ in C_{2v} geometry.

ing cross section is proportional to the principle quantum number, and to the vibrational partition of product energy,[23,24] which increases as the excitation energy of K increases. Fig. 6 displays one dimensional PES's for the Mg atom at its 4S and 3P states with H_2 under the C_{2v} symmetry. The related ionic curve Mg^+-H_2^- is also drawn by setting the H_2 electron affinity as -2.1 eV. During the early period in the reaction coordinate, $Mg(4s^1S_0) + H_2$ reaction goes forward along the slightly attractive potential surface 3^1A_1 in the entrance channel. At the crossing region, the valence electron in the quasi-Rydberg state Mg(4S) has a chance to cross to the ionic potential surface Mg^+-H_2^- because of its ionic character. A series of non-adiabatic curve crossings evolve along the Mg^+-H_2^- coordinate and finally join to the reactive 1^1B_2 surface, in which the product $MgH(X^2\Sigma^+, v'' = n)$ may be produced via a non-adiabatic transition between the 1^1B_2 surface and the ground 1^1A_1 surface. Note that the crossing region in the attractive entrance channel on the 1^1B_2 surface lies at about 2 angstroms ahead of the crossing region to the ground state surface.[7] With the aid of two dimensional potential energy surfaces, a deeper insight into the reaction pathways for the $Mg(3p^1P_1) + H_2$ reaction has been demonstrated in our previous paper.[7] The resulting PES's information reveals a non-adiabatic transition probability between the excited 1^1B_2 PES and the ground 1^1A_1 PES. The bent intermediate MgH_2 near the surface crossing may move along the trajectory smoothly following the dissociation coordinate of Mg-H distance or along the trajectory attractively falling down towards a linear HMgH geometry and giving a torque on the H end before breaking apart. The former trajectory accounts for the minor reaction pathway to produce MgH, while the latter one corresponds to the major reaction pathway.

It should be noted that the subject reaction can also occur along the slightly attractive $^1\Sigma^+$ surface in $C_{\infty v}$ symmetry in the entrance channel. It then jumps to the ionic surface and is eventually docked to the reactive 1^1B_2 surface in C_{2v} symmetry via a series of non-adiabatic curve crossings. Besides, in the process of electron transfer, the strong instability of H_2^- tends to cause most energy to be partitioned into translation. Unlike the case of the Mg(3P) state, the excitation energy facilitates Mg(4S) to undergo the pathway of electron transfer in the entrance channel, rather than to form a relatively stable insertive intermediate complex.

No apparent difference is observed in the distributions when the mass of the leaving atom is doubled. Such a lack of an isotopic effect indicates that both the low-N and high-N components may result from insertive side-on attack of the H-H bond by Mg.[4] This conclusion is also consistent with the reaction mechanism proposed above.

Similar to our work, in the $O(^1D) + CH_4$ reaction studied previously by Luntz,[25] the rotational state distributions were also characterized to be bimodal for product OH. Luntz considered that the high rotational distributions were obtained from a strong bending intermediate complex CH_3OH, when dissociating would cause a highly rotated product OH. On the other hand, the low rotational distributions were consistent with the results obtained from $O(^3P) + CH_4$ reaction. The author proposed a possibility for surface crossing between $^1A'$ and $^3A'$, by which the same intermediate route was followed and similar product rotational state distributions were produced in spite of different initial situations. Similarly, although original potential energy surfaces are different for the Mg(4s) and Mg(3p) states, they eventually all go along the same reactive route on the attractive 1^1B_2 PES, and produce similar product rotational distributions.

Similar reactions have also been found for the case of other excited alkaline earth atom with OH-containing molecules which exhibit two different mechanisms. One is the insertion mechanism via a long-lived intermediate, which may evolve to different product channels. The other follows a harpoon mechanism to form the only metal hydroxide product. For instance, in the reaction of $Ca(^1S_0, ^3P_j)$ with H_2O_2, the $Ca(^3P_j)$ atom produces CaOH, while the ground state atom leads to only CaO.[26] The corresponding pathways proceed along an insertion either into O-O or O-H bond. A competition occurs between dissociation of the intermediate complex and migration of the H atom. The reaction with $Ca(^3P_j)$ is attributed to an electron transfer, such that the ion-pair intermediate formed has no time to allow for H atom migration prior to dissociation.

CONCLUSION

We have studied the $Mg(4s^1S_0) + H_2$ reaction. The resultant rotational distributions are bimodal, with a minor component peaking at low-N and a major component peaking at high-N, and essentially consistent with those of the $Mg(3P) + H_2$ reaction. We have not found any kinematic isotopic effect on the product state distributions. The spectral analysis and potential energy surface calculations indicate that the Mg(4S) atom proceeds via a harpoon-type reaction pathway, in contrast to a direct insertion followed by Mg(3P). The Mg(4S) system is closely associated with the $Mg(3p)$-H_2 reaction coordinate, through the evolution of a series of surface crossings along the ion-pair coordinate.

ACKNOWLEDGMENT

The authors wish to thank W. T. Luh for critical reading of the manuscript. This work is financially supported by the National Science Council of the Republic of China under Contract No. NSC86-2113-M001-044-L2.

Received February 20, 1997.

Key Words

Rotational distributions; Pump-probe technique; Harpoon-type mechanism; Potential energy surface.

REFERENCES

1. Breckenridge, W. H.; Umemoto, H. *J. Chem. Phys.* **1984**, *80*, 4168.
2. McCaffery, J. G.; Parnis, J. M.; Ozin, G. A.; Breckenridge, W. H. *J. Chem. Phys.* **1985**, *89*, 4945.
3. Chaquin, P.; Sevin, A.; Yu, H. *J. Phys. Chem.* **1985**, *89*, 2813.
4. Breckenridge, W. H.; Wang, H. *Chem. Phys. Lett.* **1986**, *123*, 17; ibid **1986**, *123*, 23; ibid **1987**, *137*, 195; ibid **1987**, *139*, 28.
5. Lin, K. C.; Huang, C. T. *J. Chem. Phys.* **1989**, *91*, 5387.
6. Liu, D. K.; Chin, T. L.; Lin, K. C. *Phys. Rev. A.* **1994**, *50*, 4891.
7. Liu, D. K.; Chin, T. L.; Ou, Y. R.; Huang, C. T.; Lin, K. C. *J. Chin. Chem. Soc.* **1995**, *42*, 293.
8. Lin, K. C.; Chang, H. C. *J. Chem. Phys.* **1989**, *90*, 6151.
9. Herzberg, G. *Spectra of Diatomic Molecules*. (Van Nostrand Reinhold, New York, **1966**).
10. Kovacs, I. *Rotational Structure in the Spectra of Diatomic Molecules*. (Akademiai Kiado, Budapest, **1969**).
11. Earls, L. T. *Phys. Rev.* **1935**, *48*, 423.
12. Balfour, W. J.; Cartwright, H. M. *Astron. Astrophs. Suppl.* **1976**, *26*, 89.
13. Dwivedi, P. H.; Lin, C. S. *J. Chem. Phys.* **1978**, *69*, 3987.
14. Frisch, M. J.; Trucks, G. W.; Head-Gordon, M.; Gill, P. M. W.; Wong, M. W.; Foresman, J. B.; Johbson, B. G.; Schlegel, H. B.; Robb, M. A.; Reploglel, E. S.; Gomperts, R.; Andres, J. L.; Raghavachari, K.; Binkley, J. S.; Gonzalez, C.; Martin, R. L.; Fox, D. J.; Defrees, D. J.; Baker, J. J. J.; Stewart, P.; Pople, J. A. *GAUSSIAN 92* (Gaussian Inc., Pittsburgh, PA 15213, USA, **1992**).
15. Sevin, A.; Chaquin, P. *Chem. Phys.* **1985**, *93*, 49.
16. Bililign, S.; Kleiber, P. D.; Kearney, W. R.; Sando, K. M. *J. Chem. Phys.* **1992**, *96*, 218.
17. Bililign, S.; Kleiber, P. D. *J. Chem. Phys.* **1992**, *96*, 213.
18. Magee, J. L.; Ri, T. *J. Chem. Phys.* **1941**, *9*, 637.
19. Karl, G.; Krvus, P.; Polanyi, J. C. *J. Chem. Phys.* **1967**, *46*, 224; ibid **1967**, *46*, 244.
20. Bauer, E.; Fisher, E. R.; Gilmore, F. R. *J. Chem. Phys.* **1967**, *51*, 4173.
21. Luo, Y. L.; Lin, K. C.; Liu, D. K.; Liu, H. J.; Luh, W. T. *Phys. Rev. A* **1992**, *46*, 3834.
22. Chang, H. C.; Luo, Y. L.; Lin, K. C. *J. Chem. Phys.* **1991**, *94*, 3529.
23. Liu, D. K.; Lin, K. C. *J. Chem. Phys.* **1996**, *105*, 9121.
24. Liu, D. K.; Lin, K. C. *J. Chem. Phys.* **1997**, *107*, xxx.
25. Luntz, A. C. *J. Chem. Phys.* **1980**, *73*, 1143.
26. Oberlander, M. D.; Kampf, R. P.; Parson, J. M. *Chem. Phys. Lett.* **1991**, *176*, 385.
27. Liu, D. K.; Lin, K. C. *Chem. Phys. Lett.* **1997**, *274*, 37.